Adsorption of Polyelectrolytes at Oppositely Charged Surfaces

Andrey V. Dobrynin, Alexander Deshkovski, and Michael Rubinstein*

Department of Chemistry, University of North Carolina, Chapel Hill, North Carolina, 27599-3290

Received August 4, 2000; Revised Manuscript Received February 21, 2001

ABSTRACT: We have developed a scaling theory of polyelectrolyte adsorption at an oppositely charged surface. At low surface charge densities, we predict two-dimensional adsorbed layers with thickness determined by the balance between electrostatic attraction to the charged surface and chain entropy. At high surface charge densities, we expect a 3-dimensional layer with a density profile determined by the balance between electrostatic attraction and short-range monomer−monomer repulsion. These different stabilizing mechanisms result in a nonmonotonic dependence of the layer thickness on the surface charge density. For adsorption of polyelectrolyte chains from salt solutions, the screening of the electrostatic repulsion between adsorbed polyelectrolyte chains results in large overcompensation of the surface charge for two-dimensional adsorbed layers. At higher salt concentrations this overcompensation of the surface charge by the 2-d adsorbed layer is independent of the original surface charge and depends only on the fraction of the charged monomers on the polyelectrolyte chains and increases with ionic strength. The polyelectrolyte surface excess in 3-d adsorbed layers increases at low ionic strength and decreases at higher ionic strength.

I. Introduction

Adsorption of charged polymers—polyelectrolytes[1,2]—on charged surfaces and interfaces is a classical problem of polymer physics and has been under extensive theoretical and experimental study for the last four decades.[3−5] The broad interest in this problem is stimulated by its tremendous importance for different areas of the natural sciences ranging from materials science to physics of disordered systems and biophysics. Advances in our understanding of this complicated problem have found their applications in bioengineering, colloid stabilization, wetting, adhesion and lubrication.

One of the first analytical calculations of the polyelectrolyte adsorption at a charged surface was performed by Wiegel.[6,7] Assuming Gaussian statistics of a polyelectrolyte chain, he calculated the adsorption threshold and the thickness of the adsorbed chain as a function of salt concentration. In the same spirit the binding of flexible macromolecules to oppositely charged cylinder was treated by Odijk.[8] The interaction between the charged monomers on the chain has been taken into account by Muthukumar[9] who considered a general case of the adsorption of a polyelectrolyte chain that can take any configuration between a self-avoiding walk and a rod, depending on the ionic strength of the solution. A scaling theory of the conformations of a weakly charged polyelectrolyte chain near a charged surface was proposed by Borisov et al.[10] It was shown that adsorption of a polyion caused by long-range attraction of charged monomers to the surface includes different stages corresponding to the rearrangement of chain conformations on different length scales. The results of this theory were recently confirmed by computer simulations.[11]

The generalization of Hoeve's theory[12] for adsorption of uncharged polymers was done by Hesselink,[13] who incorporated an electrostatic contribution into Hoeve's partition function of an uncharged adsorbing polymer and considered the total free energy of a system as a sum of electrostatic and nonelectrostatic terms. Assuming a steplike polymer density distribution in the adsorbed layer, Hesselink has calculated the adsorption isotherm and polymer surface coverage as a function of the salt concentration. The calculated isotherms have the shape of the so-called "high-affinity" isotherms. At extremely low polymer concentrations in solutions, the polymer adsorbed amount rises very steeply and levels off at a saturation value. Hesselink's theory also predicts increase of adsorption with increasing salt concentration.

The significant fraction of theoretical works dealing with multi-chain polyelectrolyte adsorption on a charged surface has been carried out within the framework of the self-consistent field (SCF) method.[4] In these theories, the polymer density distribution is coupled to the local electrostatic potential through the combination of the Poisson−Boltzmann equation and the Edwards equation describing the polymer conformations in the effective external potential. This approach was first applied by Van der Schee and Lyklema[14] and Evers et al.[15] They have shown that strong repulsion between charged monomers leads to very thin adsorbed layers. If this interaction is screened, by adding salt, the adsorbed amount increases and the adsorbed layer becomes thicker. The extension of the Van der Schee and Lyklema theory to the case of weak polyelectrolytes was done by Bohmer et al.[17]

Polyelectrolyte adsorption has also been studied using the ground-state dominance approximation of the SCF method.[18−22] The linearized solution of the Poisson−Boltzmann and diffusive equations was obtained by Varoqui et al.[18] They have considered the conformation of a weakly charged polyelectrolyte at the liquid−solid interface and calculated the adsorption isotherm and the concentration profile of the polymers near the charged interface. The numerical solution of the nonlinear Poisson−Boltzmann equation was presented by Borukhov et al.[20] These authors have calculated the concentration profile of the weakly charged polyelectrolytes between two charged surfaces. The analytical results for the polymer density profiles within the framework of linear response approximation were obtained by Chatellier and Joanny.[21] It was shown that

10.1021/ma0013713 CCC: $20.00
Published on Web 04/13/2001

the concentration profile at low salt concentrations shows damped oscillations.

Rejuvenation of the theoretical interest to the problem of polyelectrolyte adsorption in recent years[23−27] was mainly due to its importance for understanding the formation of polyelectrolyte multilayers by the successive deposition of positively and negatively charged polyelectrolytes on charged surfaces from aqueous solutions.[28,29] It is now possible to produce a sequence of hundreds of alternating polyelectrolyte layers. These experiments have raised important fundamental question about charge inversion in the adsorbed polyelectrolyte layers which is responsible for successful buildup of alternating polymer layers. The model of charge inversion for adsorption of flexible polyelectrolytes was proposed by Joanny.[23] Following the traditional route and using the Edwards mean-field equation for a polyelectrolyte chain in the effective external potential together with Poisson−Boltzmann equation, Joanny showed that the overcharging is proportional to the layer thickness and is inversely proportional to the Debye screening length.

However, it was argued recently[30−32] that the Poisson−Boltzmann description of electrostatic interactions is not applicable to a system containing multivalent ions, the best example of which are polyelectrolyte molecules. The major drawback of the Poisson−Boltzmann approach is that it fails to capture the correlations between multivalent ions. These correlation effects can become so strong that the multivalent ions form a strongly correlated Wigner liquid.[30−32] The good approximation in this case is to divide the adsorbed layer into Wigner−Seitz cells surrounding each polyelectrolyte chain.[27,33] In the framework of this approach the surface overcharging can be much larger than the bare surface charge density.[24,27] It is worth pointing out that the Wigner−Seitz cell description of solutions of macroins is not new to polymer and colloidal science. This model was proposed in the 1950s and 1960s to describe the semidilute polyelectrolyte solutions[34,35] and in the 1980s to describe charge-stabilized colloidal systems.[36,37]

In the present paper, we develop a scaling theory of polyelectrolyte adsorption at an oppositely charged surface from a dilute polyelectrolyte solutions. In our model, we used new ideas of the strong correlations in polyelectrolyte systems at low surface coverage and a mean-field approach at high polymer concentrations in the adsorbed layer. The paper is organized as follows. Section II is devoted to the adsorption of polyelectrolytes from dilute salt-free solutions and shows how the layer thickness depends on the surface charge density. In section III, we generalize our model to the solutions with finite salt concentrations. Finally, in the conclusion we discuss our results and compare the prediction of our theory with experiments.

II. Adsorption of Polyelectrolytes from Salt-Free Solutions[33]

Consider a flexible polyelectrolyte chain with degree of polymerization N, fraction of charged monomers f and bond length a in a solvent with Bjerrum length

$$l_B = e^2/\epsilon kT \tag{1}$$

The electrostatic interaction between two elementary charges e separated by the Bjerrum length l_B in the solvent with dielectric constant ϵ is equal to the thermal energy kT. In a dilute salt-free solution the charges on a chain interact with each other via unscreened Coulomb potential. This electrostatic repulsion leads to chain stretching on length scales larger than electrostatic blob[38−40] size D_e. The conformation of a chain inside the electrostatic blob is almost unperturbed by electrostatic interactions with the number of monomers in it being $g_e \approx (D_e/a)^2$ in a Θ-solvent for polymer backbone. The size of the electrostatic blob D_e containing g_e monomers can be found by comparison of the electrostatic energy of a blob $e^2 g_e^2 f^2/\epsilon D_e$ with thermal energy kT. This leads to the electrostatic blob size

$$D_e \approx a(uf^2)^{-1/3} \tag{2}$$

and the number of monomers in it

$$g_e \approx (uf^2)^{-2/3} \tag{3}$$

where $u = l_B/a$ is the ratio of the Bjerrum length l_B to the bond size a. In the absence of salt, the polyelectrolyte configuration is that of a fully extended array of N/g_e electrostatic blobs of contour length L (see Figure 1)

$$L \approx \frac{N}{g_e} D_e \approx aN(uf^2)^{1/3} \tag{4}$$

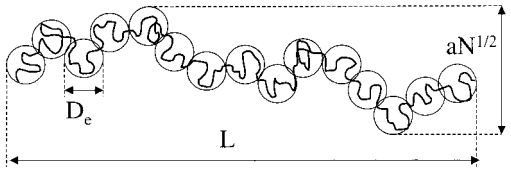

Figure 1. Polyelectrolyte chain in a dilute salt-free solution. See text for definition of length scales.

The fully extended chain of the electrostatic blobs is a fluctuating object. The typical mean-square fluctuations of the chain size in the longitudinal $\langle \delta L^2 \rangle$ and transverse $\langle R_\perp^2 \rangle$ directions are on the order of a^2N.[41]

The electrostatic self-energy of the polyelectrolyte chain W_{elec} is proportional to the thermal energy kT times the number of electrostatic blobs N/g_e in the chain

$$W_{elec} \approx kT\frac{N}{g_e} \approx kTN(uf^2)^{2/3} \tag{5}$$

A. Polyion Gouy−Chapman Preadsorption Regime. Polyelectrolyte chains replace counterions at the oppositely charged surface with the surface charge density σ. In the case of screening of the charged surface by polyions their number density profile is given by[42,43]

$$c_{ch}(z) = \frac{1}{fN}\frac{\sigma\lambda_{fN}}{(\lambda_{fN} + z)^2} \tag{6}$$

The Gouy−Chapman length λ_{fN}[42,43] for polyions with valency fN is

$$\lambda_{fN} \approx (2\pi l_B fN\sigma)^{-1} \tag{7}$$

Polyelectrolyte number density saturates near the surface

$$c_{ch} \approx \frac{\sigma}{fN\lambda_{fN}} \approx l_B\sigma^2, \quad \text{for } z < \lambda_{fN} \tag{8}$$

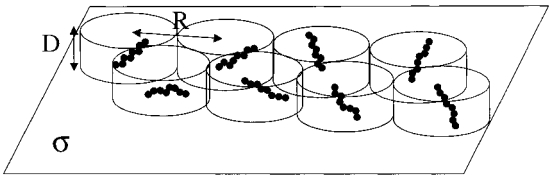

Figure 2. Schematic sketch of the adsorbed layer in the *dilute 2-d Wigner liquid* regime ($D < R$). R is the Wigner−Seitz cell size, and D is the thickness of the adsorbed layer.

Note that it is independent of chain valency fN and is the same for small counterions and large polyions. At the length scales larger than the Gouy−Chapman length the polyion density decays as z^{-2}. The mean-field picture presented above is valid as long as the thickness of the polyion Gouy−Chapman layer λ_{fN} is larger than the average distance between chains $R \approx c_{ch}^{-1/3} \approx l_B^{-1/3}\sigma^{-2/3}$ at the surface charge density below:

$$\sigma_{WC} \approx \frac{1}{l_B^2(fN)^3} \tag{9}$$

The classical Poisson−Boltzmann approach works well in the Gouy−Chapman preadsorption regime $\sigma < \sigma_{WC}$. The average repulsive energy W_{rep} between neighboring polyions

$$\frac{W_{rep}}{kT} \approx \frac{l_B(fN)^2}{R} \approx l_B^{4/3}(fN)^2\sigma^{2/3} \approx \left(\frac{\sigma}{\sigma_{WC}}\right)^{2/3} \tag{10}$$

is less than kT in this regime.

B. Dilute Two-Dimensional Wigner Liquid. a. Undeformed Polyelectrolytes. For the surface charge densities $\sigma > \sigma_{WC}$ the distance between polyions R becomes larger than their average distance to the surface $D \approx \lambda_{fN}$. In this regime, the strong electrostatic repulsion $W_{rep} \gg kT$ between chains forces them to organize into a two-dimensional strongly correlated Wigner liquid[30−32,44] at the charged surface (see Figure 2). To estimate the adsorption energy of a polyion one can consider an elementary Wigner−Seitz cell of size

$$R \approx \sqrt{\frac{fN}{\sigma}} \tag{11}$$

which is determined by the electroneutrality condition $\sigma R^2 \approx fN$ of the cell. The adsorption energy W_{ads} of the polyelectrolyte chain with the center of mass located at distance z ($z \ll R$) from the surface, is the difference between the electrostatic attraction of the polyelectrolyte chain to the charged surface and the electrostatic repulsion from all other chains. It can be estimated as the energy of electrostatic attraction between a charged disk of radius R and a charge of valency fN[30−32]

$$W_{ads}(z) \approx -kTl_BfN\sigma \int_0^R \frac{r\,dr}{\sqrt{r^2+z^2}} \approx W_{ads}(0)\left(1-\frac{z}{R}\right) \tag{12}$$

where we have introduced the adsorption energy at the surface

$$W_{ads}(0) \approx -kTl_B(fN)^{3/2}\sigma^{1/2} \approx -kT\left(\frac{\sigma}{\sigma_{WC}}\right)^{1/2} \tag{13}$$

The polyelectrolyte chains are strongly attracted to the surface with the binding energy $|W_{ads}(0)| \gg kT$ as long as the surface charge density σ is larger than the adsorption threshold value σ_{WC}. The electrostatic attraction of a polyelectrolyte chain to the charged surface $W_{ads}(0) \approx W_{elec}L/R$ is weaker than the electrostatic self-energy of a chain W_{elec} as long as polyelectrolyte chains in the adsorbed layer do not overlap ($L < R$). So, this attraction is not strong enough to perturb the internal structure of the polyelectrolyte chain determined by electrostatic repulsion between charged monomers and affects only translational and orientational degrees of freedom of the chain. The polyelectrolytes are localized within the layer of the thickness

$$D \approx R\frac{kT}{|W_{ads}(0)|} \approx (l_BfN\sigma)^{-1} \tag{14}$$

inside which (for $z < D$) the change of the adsorption energy eq 12 is on the order of the thermal energy kT. The probability to find a polyelectrolyte molecule beyond this distance D is exponentially low.[31] It is interesting to note that this length scale D is proportional to the Gouy−Chapman length λ_{fN}. The strong electrostatic attraction of a polyelectrolyte chain to a charged surface starts to affect the orientational degrees of freedom of the chain when the localization length D becomes on the order of the chain size L. This occurs at the surface charge density $\sigma \approx \sigma_L$

$$\sigma_L \approx (a^2u^{4/3}f^{5/3}N^2)^{-1} \tag{15}$$

b. Compressed Polyelectrolytes. Polyelectrolytes lay flat on the surface when the layer thickness D in eq 14 becomes comparable with the transverse size of the chains $aN^{1/2}$. This happens when the surface charge density σ reaches the value

$$\sigma_{def} \approx \frac{1}{a^2ufN^{3/2}} \tag{16}$$

At higher surface charge densities $\sigma > \sigma_{def}$, the electrostatic attraction of the charged monomers to the surface perturbs the conformations of the chains. The thickness of the chains in the direction perpendicular to the surface is determined by balancing the confinement entropy of polyelectrolyte chain kTa^2N/D^2 inside the layer of the thickness D with its electrostatic attraction $W_{ads}(D)$ (see eq 12) to the charged surface. This gives the equilibrium thickness of the chain

$$D \approx aN^{1/2}\left(\frac{\sigma_{def}}{\sigma}\right)^{1/3} \approx a^{2/3}l_B^{-1/3}f^{-1/3}\sigma^{-1/3} \tag{17}$$

that is independent of the degree of polymerization N. Chains are localized at the centers of the Wigner−Seitz cells due to strong electrostatic repulsion between them and are separated by distance $R \gg L$. A similar power law dependence of the thickness of the adsorbed layer D on the surface charge density σ was recently obtained by Borukhov et al.[22] in the framework of the Flory-like consideration of polyelectrolyte adsorption and by Borisov et al.[10] for the polyelectrolyte brushes.

c. Orientational Ordering. The effects of anisotropic shape of polyelectrolyte chains become important when the correction to the adsorption energy due to the chain anisotropy becomes on the order of the thermal energy kT. Due to the symmetry of the problem the orientation-dependent part of the electrostatic interac-

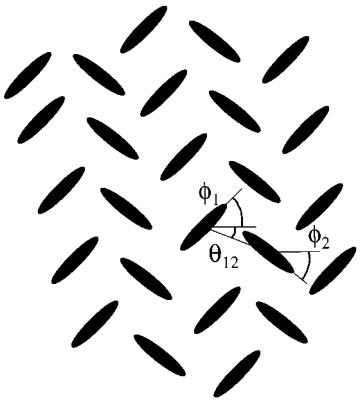

Figure 3. Ordering of polyelectrolyte chains into a herringbone structure.

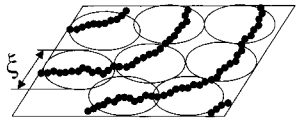

Figure 4. Schematic sketch of the adsorbed layer in the *semidilute 2-d Wigner liquid* regime.

tion between two neighboring Wigner−Seitz cells starts with quadrupole−quadrupole interactions

$$W_{\text{orient}} \approx kT\frac{l_B\sigma^{5/2}L^4}{(fN)^{1/2}}(35\cos(2\varphi_1 + 2\varphi_2 - 4\theta_{12}) + 3\cos(2\varphi_1 - 2\varphi_2)) \quad (18)$$

where φ_1 and φ_2 are the orientations of the backbones of two polyelectrolyte molecules and θ_{12} is the orientation of the vector connecting their centers (see Figure 3). The orientational transition to herringbone structure (see for review[45]) occurs at the surface charge density

$$\sigma_{\text{orient}} \approx \frac{1}{a^2u^{14/13}f^{13/15}N^{7/5}} \quad (19)$$

This is a second-order phase transition within the mean-field approximation.

C. Semidilute Two-Dimensional Wigner Liquid. As the surface charge density σ increases further, the size of the Wigner−Seitz cell $R \approx (fN/\sigma)^{1/2}$ decreases and reaches the size L of polyelectrolyte chains at the surface charge density

$$\sigma^* \approx \frac{1}{a^2u^{2/3}f^{1/3}N} \quad (20)$$

At this surface charge density the electrostatic self-energy of each chain $kTN(uf^2)^{2/3}$ becomes a value on the order of the attraction of the chain to the charged surface $W_{\text{ads}}(0)$. The adsorbed polyelectrolytes form semidilute two-dimensional strongly correlated polymeric liquid with correlation length ξ determined by the distance between sections of neighboring chains (see Figure 4). The charge of each section fg_ξ is balanced by the surface charge of the corresponding Wigner−Seitz cell $fg_\xi \approx \sigma\xi^2$. Each section still consists of an array of electrostatic blobs

$$g_\xi \approx g_e\frac{\xi}{D_e} \quad (21)$$

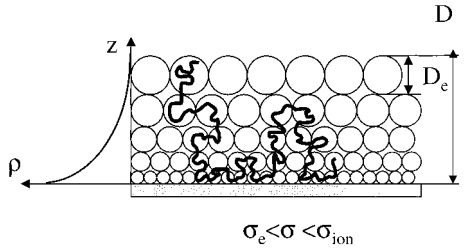

Figure 5. Polymer density profile and layer structure in the self-similar adsorbed layer.

The size of each Wigner−Seitz cell

$$\xi \approx \frac{f^{1/3}}{u^{1/3}\sigma a} \quad (22)$$

is reciprocally proportional to the surface charge density ($\xi \sim \sigma^{-1}$). At the surface charge density

$$\sigma_e \approx \frac{f}{a^2} \quad (23)$$

the size of the Wigner−Seitz cell ξ becomes on the order of the electrostatic blob size $D_e \approx a(uf^2)^{-1/3}$. At this point, the electrostatic self-energy of polyelectrolyte chain, the electrostatic attraction of this chain to the charged surface, and the confinement energy of the chain are of the same order of magnitude ($kTN(uf^2)^{2/3}$).

D. Self-Similar Adsorbed Layer. If the surface charge density increases further ($\sigma > \sigma_e$), the electrostatic attraction becomes strong enough to deform the chain on the length scales smaller than electrostatic blob size D_e. In this regime ($\sigma > \sigma_e$) the electrostatic attraction between polyelectrolytes and charged surface is balanced by the short-range repulsion between monomers (see discussion below). Near the charged surface, the polyelectrolyte chains form a concentrated polymer solution. In this regime, the distribution of the polymer density can be described in the framework of the mean-field approximation, assuming that the electrostatic interactions of polymer with the effective field created by other chains dominate over the electrostatic self-energy of the chain. Within this approximation the polymer density $\rho(z)$ and small ion density $\rho_\alpha(z)$ depend only on the distance z from the charged surface. This approximation is correct as long as the local polymer density $\rho(z)$ is higher than that inside the electrostatic blob $\rho_e \approx g_e/D_e^3 \approx a^{-3}u^{1/3}f^{2/3}$ (as in concentrated polyelectrolyte solutions).

The adsorbed layer can be considered to be built of blobs with gradually increasing size $\xi(z)$ (see Figure 5). The number of monomers $g(z)$ in a blob is determined from the fact that these blobs are space-filling $g(z) \approx \rho(z)\xi^3(z)$ and the statistics of the chain inside a blob is Gaussian $\xi^2(z) \approx a^2g(z)$. The size of the space-filling blobs in a Θ-solvent is the length scale at which three-body interaction energy is on the order of kT. These blobs are multivalent sections of polyions with the valency $fg(z)$. Each blob interacts with the external electrostatic potential $\varphi(z)$ with the energy on the order of thermal energy kT.

$$fg(z)\varphi(z) \approx 1 \quad (24)$$

This allows us to write the relation between the monomer concentration $\rho(z)$ and the electrostatic po-

tential $\varphi(z)$ at distance z from the surface

$$\rho(z) \approx g(z)/\xi^3(z) \approx a^{-3}(f\varphi(z))^{1/2} \tag{25}$$

The electrostatic potential satisfies the Poisson equation

$$\frac{d^2\varphi(z)}{dz^2} = 4\pi l_B f\rho(z) \approx ua^{-2}f^{3/2}\varphi(z)^{1/2} \tag{26}$$

together with the boundary condition at the charged surface

$$\frac{d\varphi(z)}{dz}\Big|_{z=0} = -4\pi l_B\sigma \tag{27}$$

The solution of the second-order differential equation, eq 26, is the parabolic polymer density profile (see Appendix for details)

$$\rho(z) \approx \frac{uf^2(D-z)^2}{a^5} \tag{28}$$

where the thickness of the adsorbed layer D is obtained form the boundary condition in eq 27

$$D \approx a^{5/3}u^{-1/3}f^{-1}\sigma^{1/3} \approx D_e\left(\frac{\sigma}{\sigma_e}\right)^{1/3} \tag{29}$$

The thickness of the adsorbed layer increases with increasing surface charge density σ.[23,33] The density profile in eq 28 is self-similar (power law) from the outer edge $z = D$ inward (toward the adsorbing surface). This parabolic density profile gives the following dependence of the blob size

$$\xi(z) \approx \frac{a^3}{uf^2(D-z)^2} \tag{30}$$

and the number of monomers in a concentration blob

$$g(z) \approx \frac{a^4}{u^2f^4(D-z)^4} \tag{31}$$

at distance z from the surface.

The divergence of the blob size $\xi(z)$ and the number of monomers $g(z)$ at the edge of the adsorbed layer ($z \approx D$) is due to the fact that we have neglected the polymer entropy term (see Appendix). This term suppresses large variations of monomer density at the edge of the adsorbed layer. The entropic effects begin to dominate over the three-body repulsion at distances z from the surface larger than $D - D_e$. The effective surface charge density $\Delta\sigma$ that the last layer of the thickness D_e feels is on the order of the threshold value $\sigma_e \approx fa^{-2}$. The structure of this layer is a two-dimensional melt of electrostatic blobs for which the electrostatic attraction to the surface is of the same order of magnitude as the electrostatic self-energy, confinement energy and thermal energy kT. Thus, the approximation of dominance of the three-body interactions is correct for the layer thickness D larger than electrostatic blob size D_e corresponding to the surface charge densities σ larger than σ_e

The parabolic density profile is incorrect near a charged surface where the polymer density at the impenetrable wall goes to zero. However, close to the charged surface we have a concentrated polymer solution with typical density fluctuations suppressed on length scales on the order of the correlation length $\xi \approx (\rho a^2)^{-1}$. Thus we can estimate the thickness of the polymer depletion layer to be on the order of $\xi \approx \xi(0) \approx a^{-1/3}u^{-1/3}\sigma^{-2/3}$. This layer is negligeable as long as the correlation length $\xi(0)$ is smaller than the thickness of the adsorbed layer D or for the surface charge densities σ larger than σ_e.

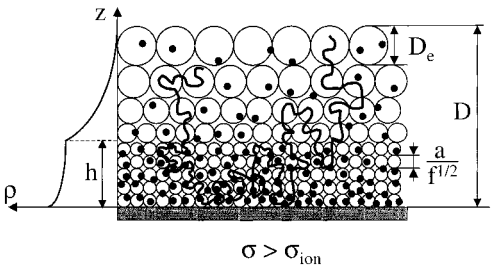

Figure 6. Polymer density profile and layer structure in the saturated self-similar adsorbed layer.

E. Saturated Self-Similar Adsorbed Layer. The number of monomers per blob in the layer closest to the surface

$$g(0) \approx \frac{\xi(0)^2}{a^2} \approx a^{-8/3}u^{-2/3}\sigma^{-4/3} \tag{32}$$

decreases with increasing surface charge density. There will be, on average, one charged monomer per such blob at the surface charge density

$$\sigma_{ion} \approx \frac{f^{3/4}}{a^2u^{1/2}} \tag{33}$$

At this surface charge density the concentration of charged monomers at the surface reaches its maximum possible value $f\rho_{max} \approx a^{-3}f^{3/2}$. Further increase of polymer density is unfavorable due to the high cost of the short-range monomer−monomer repulsive interactions. For higher surface charge densities, $\sigma > \sigma_{ion}$, surface counterions dominate the screening of the surface potential inside the layer of thickness h. A counterion pays on the order kT of the translational entropy[46] when it is localized at surface inside the layer of thickness h, while it will cost more than kT of the repulsive energy between monomers to produce a similar screening effect by increasing concentration above ρ_{max}.

To obtain analytical expressions for polymer and surface counterion density distributions, we will divide the adsorbed layer into two regions. Inside the inner region ($0 < z < h$) of the thickness h (see Figure 6) the screening of the surface electric field is dominated by surface counterions with density distribution given by[42,43]

$$\rho_{ion}(z) = \frac{1}{2\pi l_B}(z+\lambda)^{-2}, \quad \text{for } 0 < z < h \tag{34}$$

Counterions localized inside this layer reduce the surface charge density σ down to the value σ_2 that determines the boundary condition for the nonlinear equation 26 in the outer region ($h < z < D$).

$$\frac{d\varphi(z)}{dz}|_{z=h} = -4\pi l_B \sigma_2 \quad (35)$$

The electrostatic potential in the inner region ($0 < z < h$) has logarithmic form[42,43]

$$\varphi_I(z) = \varphi_0 - 2\ln\left(1 + \frac{z}{\lambda}\right), \quad \text{for } 0 < z < h \quad (36)$$

At the region boundary ($z = h$) the derivative of the electrostatic potential $\varphi(z)$ has to be continuous. The continuity of the electrostatic potential at the boundary between the two regions determines the relation between the layer thickness h, the Gouy−Chapman length λ in the inner region and λ_2 in the outer one.

$$\lambda_2 = \lambda + h \quad (37)$$

The polymer density profile inside the inner region has a weak logarithmic dependence on the distance z from the charged surface

$$\rho(z) \approx a^{-3} f^{1/2} \sqrt{\varphi_0 - 2\ln\left(1 + \frac{z}{\lambda}\right)}, \quad \text{for } 0 < z < h \quad (38)$$

The screening of the charged surface in the outer region is controlled by adsorbed polyelectrolytes. The solution of eq 26 still gives the parabolic polymer density profile

$$\rho(z) \approx \frac{u f^2 (D_{\sigma_2} + h - z)^2}{a^5}, \quad \text{for } h < z < D \quad (39)$$

with the thickness D_{σ_2} of the outer region given by eq 29 where the surface charge density σ has to be substituted by the effective surface charge density σ_2 at the region boundary ($z = h$). We have defined the zone boundary as the plane where the local concentration of the surface counterions $\rho_{ion}(h)$ is equal to the concentration of the charged monomers $f\rho(h)$.

$$\frac{1}{2\pi l_B \lambda_2^2} \approx \frac{u f^3 D_{\sigma_2}^2}{a^5} \quad (40)$$

Solving eqs 37 and 40, one can find the effective surface charge density σ_2

$$\sigma_2 \approx \frac{f^{3/4}}{u^{1/2} a^2} \approx \sigma_{ion} \quad (41)$$

The total thickness D of the polymer adsorbed layer is the sum of the thicknesses h of the inner region and D_{σ_2} of the outer one.

$$D \approx h + D_{\sigma_2} \approx \frac{a}{u^{1/2} f^{3/4}} \quad (42)$$

This layer thickness saturates at $a/u^{1/2}f^{3/4}$ for high surface charge densities $\sigma \gg \sigma_{ion}$.

Figure 6 shows the polymer density profile and the structure of the adsorbed layer in this regime. At length scales $z < h$, the monomer density ρ inside this layer is almost constant (up to logarithmic corrections) and is equal to $a^{-3}f^{1/2}$. At length scales $z > h$, the screening of the surface charge is dominated by charged monomers which results in a self-similar structure of polyelectrolyte chains with the parabolic density profile (see eq 39).

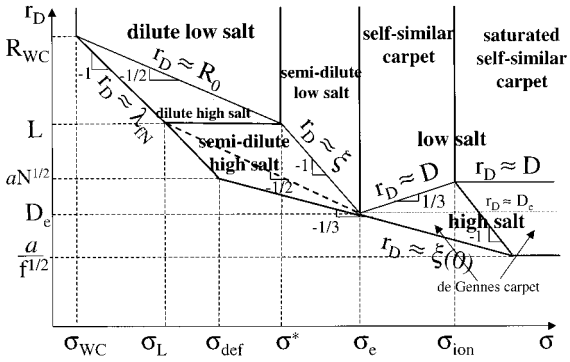

Figure 7. Adsorption diagram of polyelectrolyte chains in a salt solution as a function of surface charge density σ and Debye radius r_D.

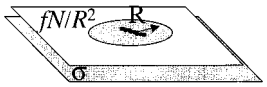

Figure 8. Schematic sketch of a polyelectrolyte chain and surrounding media for calculation of the Wigner−Seitz cell size in the *dilute 2-d Wigner liquid* regime.

At very high surface charge densities the thickness of the polymer layer saturates at $au^{-1/2}f^{-3/4}$.

III. Effects of the Added Salt on Polyelectrolyte Adsorption

In the previous sections, we have discussed various regimes of polyelectrolyte adsorption from salt-free solutions. The addition of univalent salt at concentration ρ_{salt} leads to the screening of electrostatic interactions at the Debye screening length

$$r_D = (8\pi l_B \rho_{salt})^{-1/2} \quad (43)$$

In Figure 7 we sketch the adsorption diagram of polyelectrolyte chains at an oppositely charged surface.

A. Two-Dimensional Dilute Wigner Liquid. a. Undeformed Polyelectrolytes. The total electrostatic energy of an adsorbed polyelectrolyte chain includes the electrostatic attraction of the chain to the charged surface with surface charge density σ (see Figure 8)

$$\frac{W_{att}}{kT} \approx -l_B f N \sigma \int_0^\infty dr \exp\left(-\frac{r}{r_D}\right) \approx -l_B f N \sigma r_D \quad (44)$$

and repulsion from other adsorbed polyelectrolytes distributed with effective surface charge density fN/R^2 starting at distance R from a given polyion

$$\frac{W_{rep}}{kT} \approx \frac{l_B (fN)^2}{R^2} \int_R^\infty dr \exp\left(-\frac{r}{r_D}\right) \approx \frac{l_B (fN)^2 r_D}{R^2} \exp\left(-\frac{R}{r_D}\right) \quad (45)$$

The total electrostatic energy of the adsorbed layer with the surface area S is the sum of the contributions from all chains

$$\frac{W}{kT} \approx S l_B r_D f N \left(\frac{1 fN}{2 R^4} \exp\left(-\frac{R}{r_D}\right) - \frac{\sigma}{R^2}\right) \quad (46)$$

The dependence of the Wigner−Seitz cell size R on the salt concentration is derived by minimizing the total electrostatic energy with respect to R. The equilibrium

cell size is the solution of the following equation:

$$\frac{fN}{R^2}\exp\left(-\frac{R}{r_D}\right)\left(1+\frac{1}{4}\frac{R}{r_D}\right)\approx\sigma \quad (47)$$

At low salt concentrations $r_D > \sqrt{fN/\sigma}$, the size R of the Wigner−Seitz cell has a very weak dependence on the Debye screening length r_D. It becomes approximately twice as small as the one in the salt-free case at the Debye radius $r_D \approx \sqrt{fN/\sigma}$. Thus, on the scaling level, we can assume that at low salt concentrations

$$R \approx R_0 \approx \sqrt{fN/\sigma}, \quad \text{low salt } r_D > \sqrt{fN/\sigma} \quad (48)$$

At low salt concentrations we can expand the lhs of the eq 47 in the power series of R/r_D. After this expansion, eq 47 reduces to

$$\frac{fN}{R^2}\left(1-\frac{3}{4}\frac{R}{r_D}\right)\approx\sigma \quad (49)$$

Within this approximation, the overcharging of the charged surface by adsorbed polyelectrolyte chains is

$$\delta\sigma \approx \frac{fN}{R^2}-\sigma \approx \frac{3}{4}\frac{fN}{Rr_D}\approx\frac{\sqrt{fN\sigma}}{r_D} \text{ low salt } r_D > \sqrt{fN/\sigma} \quad (50)$$

It follows from this equation that the effective surface charge density $\delta\sigma$ at the crossover between low and high salt regimes (at $r_D \approx R_0 \approx \sqrt{fN/\sigma}$ (see the crossover line in Figure 7)) is on the order of the bare surface charge density σ, but has opposite sign.

When the Debye radius r_D becomes smaller than $\sqrt{fN/\sigma}$ the adsorbed polyelectrolyte chain interacts only with the part of the surface within the Debye screening length r_D. The Wigner−Seitz cell size R that minimizes the total electrostatic energy eq 46 is

$$R \approx r_D \ln\left(\frac{fN}{\sigma {r_D}^2}\right), \quad \text{high salt } r_D < \sqrt{fN/\sigma} \quad (51)$$

Thus, up to logarithmic prefactor the cell size R is proportional to the Debye radius r_D.[27] The effective surface charge density in this high salt concentrations regime is

$$\delta\sigma \approx \frac{fN}{R^2}-\sigma \approx \frac{fN}{\left(r_D \ln\left(\frac{fN}{\sigma {r_D}^2}\right)\right)^2}\approx\frac{fN}{{r_D}^2}, \quad \text{high salt } r_D < \sqrt{fN/\sigma} \quad (52)$$

and can be much larger than the bare surface charge density σ.

As the salt concentration increases further, the Debye radius decreases and the attractive energy of the polyelectrolyte chain to the charged surface $-l_B fN\sigma r_D$ decreases as well. Polyelectrolyte chains desorb from the charged surface when the attractive energy of the chain becomes on the order of the thermal energy kT. This occurs when the Debye radius r_D becomes on the order of the Gouy−Chapman length of multivalent polyelectrolytes λ_{fN}. The line

$$r_D \approx \lambda_{fN} \approx (l_B fN\sigma)^{-1} \quad (53)$$

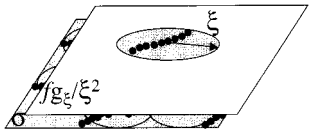

Figure 9. Schematic sketch of a section of polyelectrolyte chain and surrounding media for calculation of the Wigner−Seitz cell size in the *semidilute 2-d Wigner liquid* regime.

defines the desorption threshold for nonoverlapping polyelectrolyte chains (*dilute 2-d Wigner liquid regime*) in Figure 7. Note that in this regime the adsorbed polyelectrolyte chains are localized within the thickness $D \approx 1/(l_B fN\sigma)$ inside which the change of the adsorption energy in eq 12 is on the order of the thermal energy kT.

b. Compressed Polyelectrolytes. In this regime, the adsorbed polyelectrolyte chains are squashed by the strong attraction to the charged surface within the layer of the thickness $D \approx a^{2/3} l_B^{-1/3} f^{-1/3} \sigma^{-1/3}$. However other characteristics of the adsorbed layer like, the Wigner−Seitz cell size R and surface overcharging $\delta\sigma$, in this regime are similar to the ones obtained for *undeformed polyelectrolytes* regime.

c. Orientational Ordering. In the presence of salt, the quadrupole−quadrupole interactions between two neighboring adsorbed chains is exponentially screened at distances larger than the Debye radius r_D

$$\frac{W_{\text{orient}}}{kT}\approx\frac{l_B (fN)^2 L^4}{R^5}\exp\left(-\frac{R}{r_D}\right)(35\cos(2\varphi_1+2\varphi_2-4\theta_{12})+3\cos(2\varphi_1-2\varphi_2)) \quad (54)$$

The cell size R is given by eq 51 for high salt and by eq 48 for low salt concentrations. The orientational transition to the herringbone structure (see Figure 3) occurs when the orientational interaction W_{orient} becomes on the order of the thermal energy kT. This takes place for high salt concentrations at the Debye radius

$$r_D^{\text{orient}} \approx (l_B fNL^4\sigma)^{1/3} \approx a^{5/3} u^{7/9} f^{11/9} N^{5/3} \sigma^{1/3}, \text{ high salt } r_D < \sqrt{fN/\sigma} \quad (55)$$

For low salt concentrations, the transition is independent of salt concentrations and occurs at the surface charge density given by eq 19.

The surface overcharging and the dependence of Wigner−Seitz cell size on salt concentration in *dilute low salt* and *high salt 2-d Wigner liquid* regimes are similar to the case of adsorption of multivalent ions at oppositely charged surfaces considered by Nguyen et al.[27]

B. Two-Dimensional Semidilute Wigner Liquid. At low salt concentrations ($r_D > \xi$), the chains begin to overlap at similar surface charge densities $\sigma \approx \sigma^*$ as in the case with no added salt (see section II.C). For higher surface charge densities ($\sigma > \sigma^*$) the adsorbed polyelectrolytes arranged in a two-dimensional semidilute polyelectrolyte solution with the distance between chains $\xi \approx f^{1/3}/(u^{1/3}\sigma a)$. To calculate the total energy of the adsorbed layer, we will once again divide the electrostatic contribution to the total electrostatic energy into the repulsive and attractive ones (see Figure 9). The electrostatic energy of the adsorbed layer is

$$\frac{W}{kT} \approx S l_B r_D f g_\xi \left(\frac{f g_\xi}{2\xi^4} \exp\left(-\frac{\xi}{r_D}\right) - \frac{\sigma}{\xi^2} \right) \quad (56)$$

Minimizing the electrostatic energy of the adsorbed layer W with respect to the Wigner−Seitz cell size ξ and keeping in mind that $g_\xi \approx \xi/(f^{2/3} a u^{1/3})$, we obtain the equation that defines the cell size as a function of the Debye radius r_D

$$\frac{f^{1/3}}{u^{1/3}\xi a}\left(1 + \frac{\xi}{2r_D}\right) \exp\left(-\frac{\xi}{r_D}\right) \approx \sigma \quad (57)$$

At low salt concentrations ($r_D > \xi$) the size of the cell

$$\xi \approx \frac{f^{1/3}}{u^{1/3} a \sigma}, \quad \text{low salt } r_D > f^{1/3}/(u^{1/3} a \sigma) \quad (58)$$

is inversely proportional to the surface charge density σ, and the surface overcharging $\delta\sigma$ in this regime is

$$\delta\sigma \approx \sigma \left(\frac{\xi}{r_D}\right) \approx \frac{f^{1/3}}{u^{1/3} r_D a}, \quad \text{low salt } r_D > f^{1/3}/(u^{1/3} a \sigma) \quad (59)$$

It is inversely proportional to the Debye radius r_D and is independent of the surface charge density σ.

For high salt concentrations the solution of eq 57 is

$$\xi \approx r_D \ln\left(\frac{f^{1/3}}{\sigma r_D a u^{1/3}}\right), \quad \text{high salt } r_D < f^{1/3}/(u^{1/3} a \sigma) \quad (60)$$

The surface overcharging by the adsorbed polyelectrolyte chains at high salt concentrations

$$\delta\sigma \approx \frac{f g_\xi}{\xi^2} - \sigma \approx \frac{f^{1/3}}{u^{1/3} a r_D \ln\left(\frac{f^{1/3}}{\sigma r_D a u^{1/3}}\right)} \approx \frac{f^{1/3}}{u^{1/3} a r_D}, \text{ high salt } r_D < f^{1/3}/(u^{1/3} a \sigma) \quad (61)$$

has the same functional form as one for low salt concentrations, eq 59 (up to logarithmic corrections).

It turns out that the results for surface overcharging for flexible polyelectrolytes, obtained above (see eqs 59 and 61), are similar to the ones obtained for rigid polyelectrolytes in refs 24 and 27. This is not surprising, because the strong intrachain electrostatic repulsions between charged monomers stiffen the chains on the length scales larger than electrostatic blob size D_e and smaller than the cell size ξ. On these length scales ($D_e < r < \xi$) the chains can be considered as rodlike. The surface overcharging is determined by chain properties on scales up to cell size ξ.

Each section of the chain of size $\xi \approx r_D$ is localized within the layer of thickness $D \approx (f g_\xi \sigma l_B)^{-1} \approx (f^{1/3} u^{2/3} \sigma r_D)^{-1}$. A section lays flat on the surface when the thickness D becomes on the order of the size of the section $a\sqrt{g_\xi}$ in the direction perpendicular to the charged surface at the value of the Debye radius r_D on the order of

$$r_D^{\text{def}} \approx \sigma^{-2/3} l_B^{-1/3} \quad (62)$$

For salt concentrations such that $r_D > r_D^{\text{def}}$, the electrostatic attraction between the charged surface and the polymer chain perturbs the conformations of the section with g_ξ monomers. The thickness of the chain in the direction perpendicular to the surface is determined by the balance of the confinement entropy of the section $kTa^2 g_\xi/D^2$ inside the layer of the thickness D with its electrostatic attraction $kTl_B \sigma f g_\xi D$ to the charged surface. This leads to the equilibrium thickness D of the section given by eq 17.

Desorption of Polyelectrolyte Chains. To estimate the desorption threshold, we have to know the dependence of persistence length of polyelectrolyte chain on salt concentration that determines the size of an effective chain segment interacting with the adsorbing surface. The dependence of electrostatic persistence length on salt concentration is a controversial subject of polymer physics and is far from complete resolution. The electrostatic persistence length is found to have quadratic,[47−52] linear,[53−66] or even sublinear[67] dependences on the Debye screening length. In the present paper, we compare the results for the desorption threshold for two different dependences of the electrostatic persistence length on Debye screening length (quadratic and linear).

According to the Odijk−Skolnick−Fixman theory of the electrostatic persistence length l_p due to intrachain electrostatic repulsion is proportional to the square of the Debye radius r_D.[47,48] For weakly charged polyelectrolytes the proportionality coefficient is D_e^{-1}.[49−51]

$$l_p \approx r_D^2/D_e$$

The electrostatic attraction between the charged surface and the section of the chain of the size l_p is

$$W_{ads} \approx -kTl_B \sigma f g_\xi l_p \approx -kTuf\sigma r_D^3 a^{-1}, \quad \text{for } l_p \approx r_D^2/D_e \quad (63)$$

The desorption transition will occur when the electrostatic attraction W_{ads} of a persistence segment to the charged surface becomes on the order of thermal energy kT.[68] This condition is satisfied for the Debye screening length

$$r_D^{\text{des}} \approx \left(\frac{a}{uf\sigma}\right)^{1/3}, \quad \text{for } l_p \approx r_D^2/D_e \quad (64)$$

The crossover to rigid chain behavior occurs when the electrostatic persistent length l_p is on the order of the chain size L. This takes place at the value of the Debye radius r_D proportional to the Gaussian chain size $a\sqrt{N}$. For larger values of the Debye radius, the chain can be viewed as a linear array of electrostatic blobs of length L. The desorption of such array of blobs occurs along the desorption line given by eq 53.

However, some computer simulations of weakly charged polyelectrolyte chains[64−66] and some experiments[53−60] as well as analytical calculations[9,61−63] indicate that the exponent for the dependence of electrostatic persistent length on the Debye screening length is closer to 1 rather than to 2. The desorption transition for intrinsically flexible polyelectrolyte chain with the persistent length $l_p \approx r_D$ takes place when the electrostatic attraction of the segment of the chain of size r_D to charged surface

$$W_{ads} \approx -kTl_B \sigma f g_\xi r_D \approx -kTu^{2/3} f^{1/3} \sigma r_D^2 \quad (65)$$

becomes on the order of thermal energy kT. This

happens for the Debye screening length

$$r_D^{\text{des}} \approx (u^{2/3} f^{1/3} \sigma)^{-1/2}, \quad \text{for } l_p \approx r_D \tag{66}$$

This transition line can be viewed as the upper bound for the desorption threshold.

In Figure 7, the solid line corresponds to the desorption threshold calculated for polyelectrolyte chains with electrostatic persistence length $l_p \approx r_D^2/D_e$ and the dashed line is for chains with $l_p \approx r_D$. It is important to point out that the dependence of the chain persistence length on the Debye radius r_D is only important for calculation of the adsorption−desorption threshold for two-dimensional semidilute high salt regime and does not influence the crossover lines between other regimes of the adsorption diagram in Figure 7.

C. Low Salt Self-Similar Adsorbed Layer. In this regime, the adsorbed polymer layer is built of the blobs with gradually increasing size. In this self-similar layer the relation between the local polymer concentrations and the value of the electrostatic potential is given by eq 25. The density distribution of the salt ions in the adsorbed layer satisfies the Boltzmann distribution

$$\rho_{\pm}(z) = \rho_{\text{salt}} \exp(\mp\varphi(z)) \tag{67}$$

The Poisson equation (eq 26) in the presence of salt ions has the form

$$\frac{d^2\varphi(z)}{dz^2} = 4\pi l_B(f\rho(z) + \rho_-(z) - \rho_+(z)) \approx \frac{\varphi(z)}{r_D^2} + 4\pi\frac{uf^{3/2}}{a^2}\varphi(z)^{1/2} \tag{68}$$

The polymer density profile in the adsorbed layer in this regime is (see also Appendix for details)

$$\rho(z) = a^{-3}\sqrt{f\varphi(z)} = \frac{16\pi}{3}\frac{uf^2 r_D^2}{a^5}\sinh^2\left(\frac{D-z}{4r_D}\right) \tag{69}$$

where the thickness of the adsorbed layer D can be found from the boundary condition, eq 27.

$$\frac{64\pi}{9}\frac{uf^3 r_D^3}{a^3}\sinh^3\left(\frac{D}{4r_D}\right)\cosh\left(\frac{D}{4r_D}\right) = \sigma a^2 \tag{70}$$

In the limit $D \ll r_D$, we recover the result $D \approx a^{5/3}u^{-1/3}f^{-1}\sigma^{1/3}$ given by eq 29. The dependence of the blob sizes on the distance z from the surface is given by the following equation:

$$\xi(z) \approx \frac{a^3}{uf^2 r_D^2}\sinh^{-2}\left(\frac{D-z}{4r_D}\right) \tag{71}$$

The surface undercharging by adsorbed polyelectrolytes is obtained by integration of the polymer density profile $\rho(z)$ through the layer thickness D

$$\delta\sigma_D = f\int_0^D \rho(z)\,dz - \sigma = \sigma\left(\frac{3}{4}\frac{\sinh(y/2) - y/2}{\sinh^3(y/4)\cosh(y/4)} - 1\right) \approx -\frac{1}{20}\frac{a^{10/3}\sigma^{5/3}}{u^{2/3}f^2 r_D^2} \tag{72}$$

where $y = D/r_D$. The addition of salt decreases the polymer adsorbed amount, because salt ions also take part in screening of the surface charge. The power law dependence of the polymer surface excess on the salt concentration can be understood from following simple arguments. The typical excess charge density $\delta\rho_{\text{salt}}$ of the salt ions in the adsorbed layer is

$$\delta\rho_{\text{salt}}(z) \approx \rho^-(z) - \rho^+(z) \approx \rho_{\text{salt}}\varphi(z) \tag{73}$$

where $\varphi(z)$ is the value of the electrostatic potential at distance z from the charged surface. A typical value of the electrostatic potential $\varphi(z)$ in the adsorbed layer can be estimated as $l_B\sigma D$. Multiplying the excess charge density $\delta\rho_{\text{salt}}$ by the layer thickness D one obtains the counterion surface excess

$$\Gamma_{\text{salt}} \approx \delta\rho_{\text{salt}} D \approx l_B\rho_{\text{salt}}\sigma D^2 \approx \sigma\frac{D^2}{r_D^2} \tag{74}$$

Thus the part $\sigma D^2/r_D^2$ of the surface charge is screened by the salt ions that leaves for polyelectrolyte chains only the $\sigma - \sigma D^2/r_D^2$ part of the surface charge to screen.

However, the mean-field description of the polyelectrolyte adsorbed layer, presented above, is incorrect within distance D_e from the outer boundary of the adsorbed layer. At these distances the fluctuations of the polymer density $a^{-3}(uf^2)^{1/3}$ become larger than the average polymer density given by eq 69. This layer can be considered as a two-dimensional melt of electrostatic blobs of size D_e. The surface overcharging due to this strongly fluctuating outer layer of electrostatic blobs can be estimated by comparing the attraction of the blobs to the charge surface with electrostatic repulsion between them. The effective surface charge density $\Delta\sigma$ that the last layer of the thickness D_e feels is on the order of the threshold value $\sigma_e \approx fa^{-2}$. The attraction energy of an electrostatic blob to the charged background with the surface charge density σ_e is

$$W_{\text{att}} \approx -kTl_B\sigma_e D_e f g_e \approx -kT \tag{75}$$

The repulsion of the blob from all other blobs in this layer with the effective surface charge density $\delta\sigma_{D_e}$ is

$$W_{\text{rep}} \approx kTl_B\delta\sigma_{D_e} f g_e r_D \tag{76}$$

At equilibrium the total energy per blob in the adsorbed layer $W_{\text{att}} + W_{\text{rep}}$ is equal to the chemical potential of electrostatic blob in the bulk $kTg_eN^{-1}\ln(\rho/N) + kT \approx kT$. Thus the surface overcharging due to this last layer of electrostatic blobs is

$$\delta\sigma_{D_e} \approx \sigma_e\frac{D_e}{r_D} \approx \frac{f^{1/3}}{u^{1/3}ar_D} \tag{77}$$

Another derivation of this result is given in the Appendix.

The total overcharging of the adsorbing surface by polyelectrolyte chains is

$$\delta\sigma \approx \delta\sigma_{D_e} + \delta\sigma_D \approx \sigma_e\frac{D_e}{r_D} - \sigma\frac{D^2}{r_D^2} \tag{78}$$

The overcharging is equal to zero both in solutions with no added salt ($r_D = \infty$) and for

$$r_D^0 \approx \frac{\sigma D^2}{\sigma_e D_e} \approx \frac{a^{13/3}\sigma^{5/3}}{u^{1/3}f^{7/3}} \approx D_e\left(\frac{\sigma}{\sigma_e}\right)^{5/3} \tag{79}$$

At very low salt concentrations ($r_D > r_D^0$), the surface is overcharged by the adsorbed 3-d layer. At higher salt concentrations ($r_D < r_D^0$) the net charge of the adsorbed polyelectrolyte chains becomes smaller than the bare surface charge σ. The surface undercharging by adsorbed polyelectrolyte chains is on the order of the bare surface charge density σ when the Debye screening length r_D is comparable with the layer thickness D.

$$r_D^D \approx D \approx a^{5/3}u^{-1/3}f^{-1}\sigma^{1/3} \tag{80}$$

For higher salt concentrations the system crosses over to the *high salt self-similar adsorbed layer regime*.

D. High Salt Self-Similar Adsorbed Layer. At high salt concentrations the solution of eq 70 is

$$D \approx r_D \ln\left(\frac{\sigma a^5}{uf^3 {r_D}^3}\right) \tag{81}$$

and inside this layer there is still a self-similar structure of blobs with sizes given by eq 71.

The polymer surface excess Γ in this regime is the sum of two contributions which are due to the self-similar polyelectrolyte layer near the surface of size D and due to the thin layer of the size of the electrostatic blob D_e at the edge of the self-similar layer

$$\Gamma \approx \frac{\sigma}{f}\exp\left(-\frac{D}{2r_D}\right) + \frac{\sigma_e}{f}\frac{D_e}{r_D} \approx \left(\frac{\sigma u f {r_D}^3}{a^5}\right)^{1/2} \tag{82}$$

As the surface charge density increases the size of the first blob $\xi(0) \approx a^{1/2}(uf\sigma r_D)^{-1/2}$ decreases. At the surface charge density

$$\sigma_{ion}^s \approx \frac{1}{ur_D a} \tag{83}$$

the size of this blob will be on the order of the distance between charged monomers $a/\sqrt{f}$ or there will be one charged monomer per such blob. This is the maximum possible screening of the surface by polyelectrolytes. The further increase of polymer density near the surface is unfavorable due to the high cost of the short-range monomer−monomer repulsive interactions. For the higher surface charge densities $\sigma > \sigma_{ion}^s$ surface counterions start to dominate the screening of the surface potential near the surface and the system crosses over into the *high salt saturated self-similar adsorbed layer* regime.

The adsorbed layer begins to swell when the Debye radius r_D becomes smaller than the electrostatic blob size D_e. We still expect a self-similar adsorbed layer of the thickness $D \approx r_D$ (see eq 81). But in this three-dimensional adsorption regime ($\sigma > \sigma_e$) with the Debye radius $r_D < D_e$, there is also a self-similar de Gennes carpet[69] on the top of the self-similar layer of thickness r_D (see Figure 10). The density profile in this outer carpet is similar to the one for neutral polymers with excluded volume parameter $v \approx l_B {r_D}^2 f^2$ and is decaying with the distance z from the surface as $z^{-4/3}$. The

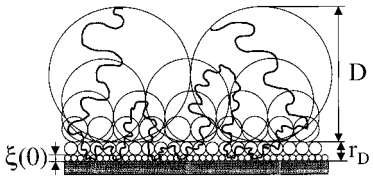

Figure 10. Schematic sketch of the self-similar adsorbed layer for $r_D < D_e$.

thickness of the adsorbed layer is on the order of the chain size

$$D \approx v^{1/5}a^{2/5}N^{3/5} \approx a^{3/5}u^{1/5}f^{2/5}{r_D}^{2/5}N^{3/5} \tag{84}$$

The desorption occurs when the size of a blob at the charged surface $\xi(0) \approx a^{1/2}(uf\sigma r_D)^{-1/2}$ becomes on the order of the Debye radius r_D. This takes place at salt concentrations for which the Debye radius

$$r_D^{des} \approx \left(\frac{a}{uf\sigma}\right)^{1/3} \tag{85}$$

It is interesting to notice that this desorption condition is identical to eq 64 for a 2-d layer with electrostatic persistence length $l_p \approx {r_D}^2/D_e$. At this value of the Debye radius $r_D \approx r_D^{des}$ the attraction energy of the blob to the surface is on the order of thermal energy kT. Our prediction for the desorption threshold in eq 85 agrees with that derived in refs 6, 7, 9, and 19 in the framework of the ground state dominance approximation.

E. Saturated Self-Similar Adsorbed Layer. In this regime, the surface counterions control the screening of the surface charge near the surface. The polymer concentration near the surface is almost constant and is equal to

$$\rho(0) \approx a^{-3}f^{1/2} \tag{86}$$

while the concentration of the surface counterions is equal to

$$\rho_{ion}(z) \simeq \frac{\sigma^2 l_B}{(1 + \sigma l_B z)^2} \tag{87}$$

The concentration of surface counterions becomes comparable with the concentration of the charged monomers $f\rho(0)$ at the length scale

$$h \approx D_{sat} \approx au^{-1/2}f^{-3/4} \tag{88}$$

At length scales $z > h$, the polyelectrolyte chains control the screening of the charged surface and the structure of the adsorbed layer is similar to that in the *self-similar layer* regimes. The polymer surface excess in this regime is

$$\Gamma \approx \begin{cases} \dfrac{1}{u^{1/2}a^2f^{1/4}} + \dfrac{1}{u^{1/3}f^{2/3}ar_D} - \dfrac{a^{10/3}}{u^{3/2}f^{7/4}{r_D}^2}, \\ \qquad\qquad \text{low salt,} \quad r_D > D_{sat} \\ \dfrac{f^{1/2}r_D}{a^3}, \quad \text{high salt,} \quad af^{-1/2} < r_D < D_{sat} \end{cases} \tag{89}$$

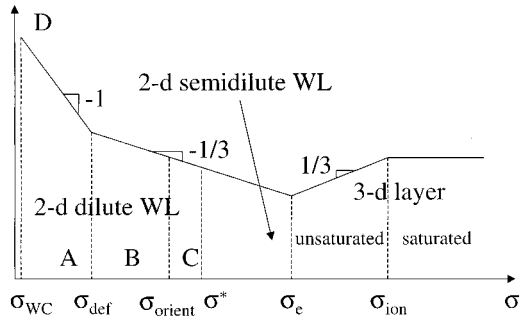

Figure 11. Dependence of the thickness of the adsorbed layer D on the surface charge density σ in salt-free solution (logarithmic scales).

The polyelectrolyte chains desorb when the Debye radius r_D becomes on the order of the distance between charged monomers $af^{-1/2}$.

IV. Discussion and Conclusion

We have presented a scaling analysis of the polyelectrolyte adsorption at oppositely charged surfaces from dilute polymer solutions. Polyelectrolytes substitute surface counterions and form a two-dimensional strongly correlated dilute Wigner liquid, Wigner liquid crystal, and semidilute two-dimensional polyelectrolyte layer at the charged surface in the case of adsorption from salt-free solutions in the interval of the surface charge densities ($\sigma_{WC} < \sigma < \sigma_e$). The size of the corresponding Wigner−Seitz cell is determined by the electroneutrality condition of the cell. The chains are localized inside the layer of thickness $D \approx (l_B f N \sigma)^{-1}$ for surface charge densities smaller than σ_{def}. For higher surface charge densities $\sigma > \sigma_{def}$, the thickness of adsorbed chains D is determined by the balance of the energy gain due to electrostatic attraction and the confinement entropy lost due to chain localization. The equilibrium chain thickness D decreases with increasing surface charge density as $\sigma^{-1/3}$. The orientational transition in the adsorbed layer at $\sigma \approx \sigma_{orient}$ and crossover into 2-d semidilute adsorbed layer at $\sigma \approx \sigma^*$ have no effect on the layer thickness (see Figure 11).

If the surface charge density increases further ($\sigma_e < \sigma < \sigma_{ion}$), the equilibrium density profile in the adsorbed layer is determined by the balance between electrostatic attraction of charged monomers to the surface and short-range monomer−monomer repulsion. On length scales $z < D - D_e$ the polyelectrolytes form a self-similar carpet with polymer density decaying as $(D - z)^2$ in a Θ-solvent for polymer backbone. The thickness of the adsorbed layer D increases with surface charge density as $\sigma^{1/3}$ (see Figure 11).

For very high surface charge densities ($\sigma > \sigma_{ion}$) the surface counterions dominate the screening of the surface potential near the wall and reduce the effective surface charge density to the crossover value σ_{ion}. The polymer density within this layer is almost constant $\rho \approx a^{-3}f^{1/2}$ with one elementary charge per correlation blob. Further away from the wall, adsorbed polyelectrolytes form a self-similar structure as described above. In this regime, the thickness of the adsorbed layer saturates at $au^{-1/2}f^{-3/4}$ (see Figure 11). It is useful to estimate the typical σ values for the boundaries between different regimes in the adsorption diagram (Figure 11). Consider polyelectrolyte chains consisting of $N \approx 10^2$ Kuhn segments with size $a \approx 4A$ and with 10% ($f \approx 0.1$) of these segments charged adsorbing from an aqueous solution with the Bjerrum length $l_B = 7A$. In this case the boundaries between regimes in the adsorption diagram are $\sigma_{WC} \approx 2 \times 10^{-5}\ A^{-2}$, $\sigma_{def} \approx \sigma_{orient} \approx 10^{-3}\ A^{-2}$, $\sigma_e \approx 6 \times 10^{-3}\ A^{-2}$, and $\sigma_{ion} \approx 10^{-2}\ A^{-2}$. Most of these regimes are within the experimental range for polyelectrolyte adsorption on glass and on mica substrates.

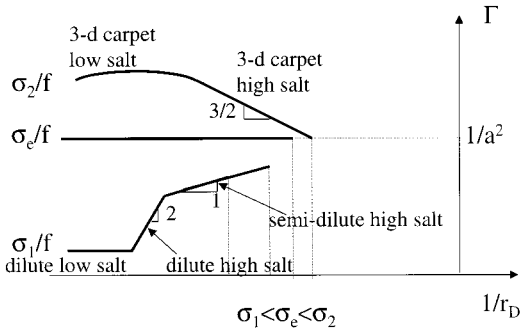

Figure 12. Dependence of polymer surface excess on salt concentration (logarithmic scales).

Addition of salt can either increase or decrease the amount of adsorbed polyelectrolytes. Figure 12 shows the dependence of the polymer surface excess

$$\Gamma \approx \frac{\sigma + \delta\sigma}{f} \tag{90}$$

on salt concentration for three different values of the surface charge density σ. For the surface charge σ_1 below σ^* the polymer surface excess increases with decreasing the Debye radius (increasing salt concentration). In this case the addition of salt decreases the repulsion between adsorbed polyelectrolyte chains promoting higher surface coverage. At very low salt concentrations the polymer surface excess Γ is equal to σ/f and adsorbed polyelectrolytes totally compensate the surface charge σ. In the *dilute low salt Wigner liquid* regime the surface overcharging $\delta\sigma$ is inversely proportional to the Debye radius r_D. Thus in this regime the polymer surface excess will increase with the salt concentration as r_D^{-1}

$$\Gamma_{DLWL} \approx \frac{\sigma}{f} + \frac{1}{r_D}\sqrt{\frac{N}{f\sigma}}, \quad \text{for } r_D > \sqrt{fN/\sigma} \tag{91}$$

The crossover into *dilute high salt Wigner liquid* regime occurs when the size of the Wigner−Seitz cell $\sqrt{fN/\sigma}$ is on the order of the Debye radius r_D. For higher salt concentrations, there is on average one polyelectrolyte chain per area r_D^2 and the polymer surface excess

$$\Gamma_{DHWL} \approx \frac{N}{r_D^2}, \quad \text{for } L < r_D < \sqrt{fN/\sigma} \tag{92}$$

increases linearly with salt concentration ρ_{salt}. The chains in the adsorbed layer start to overlap when the Debye radius r_D is on the order of the chain size L. At higher salt concentrations the system is in the *semidilute high salt 2-D Wigner liquid* regime. The polymer surface excess in this regime

$$\Gamma_{SHWL} \approx \frac{1}{u^{1/3}f^{2/3}ar_D}, \quad \text{for } r_D^{des} < r_D < L \tag{93}$$

is proportional to the square-root of salt concentration $\sqrt{\rho_{salt}}$. Qualitatively different dependence of the sur-

face coverage on salt concentration is predicted for surface charge densities $\sigma_2 > \sigma_e$. In this range of surface charge densities the adsorbed polyelectrolytes form a 3-d adsorbed layer. The addition of the salt to this system results in two opposite effects. The addition of the salt decreases the polymer adsorbed amount in the 3-d layer, because salt ions are also participating in screening of the surface charge, relieving polymers from the screening duty. However, the polymer surface excess in the thin outer layer of the size of electrostatic blob D_e increases with increasing salt concentration. In this two-dimensional outer layer, the addition of the salt reduces the electrostatic repulsion between charged monomers. The total polymer surface excess in this regime is

$$\Gamma_{LSSC} \approx \frac{\sigma}{f} - \frac{\sigma}{f}\frac{D^2}{r_D^2} + \frac{1}{a^2}\frac{D_e}{r_D}, \quad \text{for } r_D > D \qquad (94)$$

Thus the polymer surface excess first grows and then decreases as salt is added to the polyelectrolyte solution. However, the increase in the polymer surface excess will be significant only at surface charge densities very close to the boundary value σ_e. For $\sigma \gg \sigma_e$ the initial increase in the polymer surface excess Γ is relatively small. When the Debye radius becomes on the order of the layer thickness D the system crosses over into the *high salt self-similar carpet* regime. In this regime the surface excess decreases with the increasing the salt concentrations as $\rho_{salt}^{-3/4}$

$$\Gamma_{HSSC} \approx \left(\frac{\sigma u f r_D^3}{a^5}\right)^{1/2}, \quad \text{for } \left(\frac{a}{uf\sigma}\right)^{1/3} < r_D < D \qquad (95)$$

The surface coverage goes to zero at the desorption threshold.

At the crossover value σ_e of the surface charge density between the two regimes, the surface coverage $\Gamma \approx \sigma_e/f$ is independent of salt concentration (see Figure 12).

Both increase and decrease of the adsorbed amount with salt concentration for polyelectrolytes with different fraction of charged monomers f were found by Durand et al.[70] for adsorption of cationic polyacrylamides (copolymers of acrylamide and acrylate with a quaternary ammonium groups) on montmorillonite. For polyelectrolytes with fraction of charged monomers $f = 0.01$, the adsorbed amount decreases with increasing salt concentration; for $f = 0.05$, there was no salt effect, while for polyelectrolytes with $f = 0.13$ and $f = 0.3$ the adsorbed amount increases with increasing salt concentration. This trend in the dependence of the adsorbed amount on salt concentration can be rationalized in our model of polyelectrolyte adsorption. With increasing the fraction of the charged monomers f on polymer chain the crossover value $\sigma_e \approx f/a^2$ shifts into the region of high surface charge densities. Thus for small $f \leq 0.05$, the adsorbed polyelectrolytes form a 3-d adsorbed layer for which the polymer surface excess decreases with increasing the salt concentration (*screening-reduced adsorption*). Independence of the polymer surface excess on salt concentration for the sample with $f = 0.05$ indicates that the surface charge density in their experiments σ is very close to σ_e for this sample. The adsorbed polyelectrolytes form a two-dimensional adsorbed layer for fractions of charged monomers $f > 0.05$ for which the polymer surface excess increases with increasing salt concentration (*screening-enhanced adsorption*). The *screening-reduced adsorption* was also observed in other experiments on polyelectrolyte adsorption.[71−77] The *screening-enhanced adsorption* was reported by Kawaguchi et al.[78] for adsorption of completely quaternized poly(4-vinyl-*N*-*n*-propylpyridinium bromide) on silica, and by Bonekamp[79] for adsorption of polylysine onto silver-iodide crystal and on glass. The linear dependence of the polymer surface excess on the square root of salt concentration ($\Gamma \sim \sqrt{\rho_{salt}}$) was reported by Kawaguchi et al.[78] and by Marra et al.[80] for adsorption of polystyrene sulfonate on weakly charged silica at pH $\approx$ 2. This dependence of the polymer surface excess is in good qualitative agreement with our prediction for polyelectrolyte adsorption in both *low and high salt semidilute 2-d polymeric Wigner liquid* regimes, eq 93.

The nonmonotonic dependence of the polymer surface excess on the salt concentration with weak maximum around $10^{-1}-10^{-2}$ M was observed by Bonekamp[79] for adsorption of polylysine on silica at two different pH = 7.5 and 6. This is exactly what our model predicts for polyelectrolyte adsorption in the *low salt self-similar carpet* regime. This is a manifestation of the two opposite tendencies: (i) the increase of the polymer surface excess due to the screening of the electrostatic repulsion between chains in the thin outer layer of size D_e; (ii) the decrease of polymer surface excess through the 3-d adsorbed layer with thickness D due to screening of the surface charge by salt ions.

Thus our theory of polyelectrolyte adsorption on oppositely charged surface gives qualitatively correct interpretations of the experimental results using only the electrostatic nature of polyelectrolyte adsorption without invoking any additional assumptions about specific interactions of polymer backbone and salt ions with a charged surface. Of course our theory does not cover all aspects of polyelectrolyte adsorption. We leave aside the questions of (i) adsorption of weak polyelectrolytes where the actual charge fraction f is controlled by the *pH* of the solution and by the local environment, (ii) effect of specific interactions between polymer backbone and adsorbing surface, and (iii) effect of difference in the dielectric constants of solvent and adsorbing substrate on polyelectrolyte adsorption. Another problem that is not discussed in the present paper is the adsorption of polyelectrolytes from poor solvents for polymer backbone. Already in the solutions these polymers demonstrate unusual behavior—formation of the necklacelike structures[81−89]—and one can anticipate some unusual behavior of these polymers at charged surfaces as well. We will address these problems in future publications. However, despite of all these limitations, we hope our paper will serve as a springboard for future development of more sophisticated theories of polyelectrolyte adsorption.

Acknowledgment. The authors are grateful to B. Shklovskii for valuable discussions and to the National Science Foundation for financial support under Grant DMR-9730777.

Appendix

Within the mean-field approximation, the free energy of the system has three terms, which include the electrostatic interactions between counterions, polyelectrolyte chains and the surface charges, V_{elect}, the translational entropy of counterions F_{count} and the free energy

of polymer chains F_{pol}.

$$\Delta F = V_{elect} + F_{pol} + F_{count} \quad (96)$$

The part of the free energy describing the electrostatic interactions in solution, V_{elect}, is

$$\frac{V_{elect}}{kT} = -2\pi l_B \sigma S \int_0^\infty z q(z) dz - \pi l_B S \int_0^\infty \int_0^\infty |z - z'| q(z) q(z') dz\, dz' \quad (97)$$

The first term in the rhs describes the effects of electrostatic interactions between the charged surface and the charge distribution $q(z)$ in the system

$$q(z) = -f\rho(z) + \sum_\alpha q_\alpha \rho_\alpha(z) \quad (98)$$

where q_α and $\rho_\alpha(z)$ are the valency and the local density of small ions in the system and $\rho(z)$ is the local polymer concentration. The second term in the rhs of the eq 97 describes the electrostatic interactions between the charged layers located at distances z and z' from the charged surface. The polymeric contribution F_{pol} to the free energy includes three terms: the conformational entropy of the polymer chains, the third virial term describing the monomer−monomer interactions in a Θ-solvent, and the ideal gas contribution due to chains translational entropy in the adsorbed layer

$$\frac{1}{S}\frac{F_{pol}}{kT} = \frac{a^2}{6}\int_0^D \left(\frac{d}{dz}\sqrt{\rho(z)}\right)^2 dz + \frac{a^6}{3}\int_0^D \rho(z)^3\, dz + \frac{\Gamma}{N}\ln\left(\frac{\Gamma a^3}{DNe}\right) \quad (99)$$

where Γ is the polymer surface coverage

$$\Gamma = \int_0^D \rho(z)\, dz \quad (100)$$

The polyelectrolyte chains are localized within the layer of thickness D and are in the thermal equilibrium with the bulk. At equilibrium, the chemical potential of the polyelectrolyte chains in the adsorbed layer is

$$\mu_{ads} = kT \ln\left(\frac{\Gamma a^3}{DN}\right) + kTN\mu \quad (101)$$

where μ is the Lagrange multiplier for the constraint in eq 100 and is equal to the chemical potential of polyelectrolyte chains in bulk solution with polymer concentration ρ_{bulk}.

$$\mu_{ch} \approx kT \ln\left(\frac{\rho_{bulk} a^3}{N}\right) + kT\frac{N}{g_e} \quad (102)$$

The second term in the rhs of eq 96 is the self-energy of the polyelectrolyte chain in the bulk.

The nonelectrostatic contribution of the small ions to the free energy (eq 96) in our approach is taken into account on the level of their ideal gas entropy

$$\frac{1}{S}\frac{F_{count}}{kT} = \sum_\alpha \int_0^\infty \rho_\alpha(z) \ln\left(\frac{\rho_\alpha(z)}{e}\right) dz \quad (103)$$

To find the equilibrium polymer and counterion density distributions near the charged surface, we have to take the variational derivative of the free energy with respect to polymer $\rho(z)$ and small ions $\rho_\alpha(z)$ densities subject to additional constrains that fix the total number of molecules in the system. The extremal equation for the polymer density distribution is

$$\mu = a^6\rho(z)^2 - f\varphi(z) - \frac{a^2}{6}\frac{1}{\sqrt{\rho(z)}}\frac{d^2\sqrt{\rho(z)}}{dz^2} \quad (104)$$

This parameter μ can be found from the condition that at equilibrium the chemical potentials of polyelectrolyte chains in the bulk μ_{ch}, eq 102, and in the adsorbed layer μ_{ads}, eq 101, are equal. For long polyelectrolyte chains ($N \gg 1$), the parameter μ is equal to g_e^{-1} and can be considered as the chemical potential of the monomer in the bulk.

In eq 104, we have introduced the reduced electrostatic potential $\varphi(z)$

$$\varphi(z) = -2\pi l_B \sigma z - 2\pi l_B \int_0^\infty |z - z'| q(z')\, dz' \quad (105)$$

that satisfies the Poisson equation

$$\frac{d^2\varphi(z)}{dz^2} = 4\pi l_B (f\rho(z) - \sum_\alpha q_\alpha \rho_\alpha(z)) \quad (106)$$

with the boundary condition at the charged surface

$$\frac{d\varphi(z)}{dz}\Big|_{z=0} = -4\pi l_B \sigma \quad (107)$$

We will assume that there is no specific interactions between polymers and the surface except for electrostatic ones and that the surface is impenetrable for monomers. This gives us the following boundary condition for polymer concentration at the charged surface.

$$\rho(0) = 0 \quad (108)$$

The distribution of small ions in the adsorbed polymer layer is given by the Boltzmann distribution

$$\rho_\alpha(z) = \rho_\alpha \exp(-q_\alpha \varphi(z)) \quad (109)$$

where ρ_α is the bulk concentration of the small ions. Thus the system of eqs 104, 105, 106, and 109 together with the boundary conditions (eqs 107 and 108) describes polyelectrolytes adsorption from dilute polymer solution.

Self-Similar Adsorbed Layer. The system of differential equations 104−106 can be solved analytically when the screening of the charged surface is dominated by adsorbed polyelectrolyte chains and salt ions. In this case, these equations can be reduced to

$$g_e^{-1} = a^6\rho(z)^2 - f\varphi(z) - \frac{a^2}{6}\frac{1}{\sqrt{\rho(z)}}\frac{d^2\sqrt{\rho(z)}}{dz^2} \quad (110)$$

$$\frac{d^2\varphi(z)}{dz^2} - \frac{\varphi(z)}{r_D^2} = 4\pi l_B f\rho(z) \quad (111)$$

where r_D is the Debye radius due to the salt ions ($r_D^{-2} = 8\pi l_B \rho_{salt}$). In our analysis of these equations, we first ignore the last term in the rhs of eq 110 that is due to

conformational entropy of the polyelectrolyte chains and disregard the boundary condition for polymer concentration at the charged surface in eq 108. We will discuss the limitations of these approximations below. The monomer chemical potential $\mu \approx g_e^{-1}$ can be neglected if the local monomer concentration $\rho(z)$ is larger than $a^{-3}u^{1/3}f^{2/3}$. For high polymer concentrations $\rho(z) > a^{-3}u^{1/3}f^{2/3}$ we can assume that

$$a^6\rho(z)^2 \approx f\varphi(z) \tag{112}$$

and rewrite eq 111 as follows

$$\frac{d^2\varphi(z)}{dz^2} - \frac{\varphi(z)}{r_D^2} = \frac{4\pi l_B f^{3/2}}{a^3}\sqrt{\varphi(z)} \tag{113}$$

This equation is solved by the following polymer density profile

$$\rho(z) = \frac{16\pi}{3}\frac{uf^2 r_D^2}{a^5}\sinh^2\left(\frac{D-z}{4r_D}\right) \tag{114}$$

where the thickness of the adsorbed layer D can be obtained from the boundary condition in eq 107

$$\frac{64\pi}{9}\frac{uf^3 r_D^3}{a^3}\sinh^3\left(\frac{D}{4r_D}\right)\cosh\left(\frac{D}{4r_D}\right) = \sigma a^2 \tag{115}$$

For low salt concentrations ($r_D \gg D$) polymer density profile is parabolic

$$\rho(z) = \frac{\pi}{3}\frac{uf^2(D-z)^2}{a^5} \tag{116}$$

and the layer thickness D is given by the following expression:

$$D = \left(\frac{9}{\pi}\right)^{1/3} a^{5/3}u^{-1/3}f^{-1}\sigma^{1/3} \tag{117}$$

The density profile given by eq 116 is incorrect near the charged surface ($z \approx 0$) and at the edge of the adsorbed layer ($z \approx D$)—in the regions with large gradients of polymer density. Close to the charged surface, we have a concentrated polymer solution in which the typical density fluctuations occurs at the length scales on the order of the correlation length $\xi(z) \approx (\rho(z)a^2)^{-1}$. Near the charged surface, the polymer depletion layer is on the order of $\xi(0) \approx a^{1/3}u^{-1/3}\sigma^{-2/3}$. The contribution from this layer is negligeable as long as the correlation length $\xi(0)$ is smaller than the thickness of the adsorbed layer D or for the surface charge densities σ larger than f/a^2.

At the edge of the adsorbing layer the three-body interactions $a^6\rho(z)^3$ become on the order of the chain conformational entropy

$$\frac{u^3f^6(D-z)^6}{a^9} \approx a^6\rho(z)^3 \approx \frac{a^2}{6}\left(\frac{d\sqrt{\rho(z)}}{dz}\right)^2 \approx \frac{uf^2}{a^3} \tag{118}$$

at the distance z from a charged surface

$$z \approx D - a(uf^2)^{-1/3} \approx D - D_e \tag{119}$$

At these length scales we have to take into account the gradient terms in eq 110. However, the contribution from this layer can also be neglected if the thickness of the adsorbed layer D is larger than the size of the electrostatic blob D_e or $\sigma > f/a^2$.

Surface Overcharging. The polymer density profile equation, eq 114, predicts only the decrease of polymer surface excess with increasing salt concentration. To calculate the net charge of the adsorbed layer, we divided solution into two regions: region I of thickness D with the screening of surface charge due to the polyelectrolyte chains and salt ions; region II, $z > D$, with negligibly small polymer concentration and the screening of the effective surface charge exclusively by the salt ions.

In region II, the electrostatic potential satisfies the following differential equation

$$\frac{d^2\varphi_{II}(z)}{dz^2} = \frac{\varphi_{II}(z)}{r_D^2} \tag{120}$$

with the boundary condition

$$\frac{d\varphi_{II}(z)}{dz}\Big|_{z=D} = -4\pi l_B\delta\sigma \tag{121}$$

where $\delta\sigma = \sigma - f\Gamma - \Gamma_{salt}$ is the effective surface charge density to be determined by self-consistently matching the electrostatic potential and its derivative with these in the region I at the boundary of the two regions ($z \simeq D$). The positive value of $\delta\sigma$ corresponds undercharging of the charged surface. The electrostatic potential in the region II is

$$\varphi_{II}(z) = 4\pi l_B r_D\delta\sigma\exp\left(-\frac{z-D}{r_D}\right) \tag{122}$$

In region I the local electrostatic potential and polymer concentration are related through the system of equations

$$g_e^{-1} = a^6\rho(z)^2 - f\varphi_I(z) - \frac{a^2}{6}\frac{1}{\sqrt{\rho(z)}}\frac{d^2\sqrt{\rho(z)}}{dz^2} \tag{123}$$

$$\frac{d^2\varphi_I(z)}{dz^2} - \frac{\varphi_I(z)}{r_D^2} = 4\pi l_B f\rho(z) \tag{124}$$

Since we are interested in the order of magnitude estimate for the effective surface charge density $\delta\sigma$, we can estimate the terms in the last equation at $z = D$ as follows

$$g_e^{-1} \approx -4\pi f l_B\delta\sigma r_D - \frac{a^2}{6}\frac{1}{\sqrt{\rho(z)}}\frac{d^2\sqrt{\rho(z)}}{dz^2}\Big|_{z=D} \tag{125}$$

To find overcharging $\delta\sigma$, we have to estimate the second term in the rhs of eq 125. This can be done by taking the square root from both sides of eq 124 and taking the second derivative with respect to z. Once again, using the continuity condition of the electrostatic potential, we can obtain the necessary derivatives of the electrostatic potential $\varphi_I(z)$ at $z = D$ from that of the potential $\varphi_{II}(z)$ in region II.

$$g_e^{-1} \approx -4\pi f l_B\delta\sigma r_D - \frac{a^2}{24r_D^2} \tag{126}$$

Solving this equation for $\delta\sigma$, one finds

$$\delta\sigma \approx -\frac{f^{1/3}}{u^{1/3}ar_D} - \frac{a}{fur_D{}^3} \approx -\sigma_e\frac{D_e}{r_D}\left(1 + \frac{D_e{}^2}{r_D{}^2}\right) \qquad (127)$$

the surface overcharging by adsorbed polyelectrolyte chains in region I.

A somewhat different result in the framework of the similar approach for the surface overcharging $\delta\sigma$ was recently derived by Joanny.[23] He demonstrated that the surface overcharging $\delta\sigma$ is proportional to the thickness of the adsorbed layer D and is inversely proportional to the Debye radius r_D ($\delta\sigma \approx \sigma D/r_D$). We believe that the discrepancy with our result is due to constant polymer density profile in the adsorbed layer assumed in ref 23.

References and Notes

(1) *Polyelectrolytes*, M. Hara Ed.; Marcel Dekker: New York, 1993.
(2) Schmitz, K. S. *Macroions in Solution and Colloidal Suspension*; VCH: Weinheim, Germany, 1993.
(3) Kawaguchi, M.; Takahashi, A. *Adv. Colloid Interface Sci.* **1992**, *37*, 219.
(4) Fleer, G. J.; Cohen Stuart, M. A.; Scheutjens, J. M. H. M.; Gasgove, T.; Vincent, B. *Polymer at Interfaces*; Chapman and Hall: London, 1993.
(5) Bajpai, A. K. *Prog. Polym. Sci.* **1997**, *22*, 523.
(6) Wiegel, F. W. *J. Phys. A* **1977**, *10*, 299.
(7) Wiegel, F. W. In *Phase Transition and Critical Phenomena*; Domb, C., Leibowitz, J. L., Eds.; Academic: New York, 1983; Vol. 7.
(8) Odijk, T. *Macromolecules* **1980**, *13*, 1542.
(9) Muthukumar, M. *J. Chem. Phys.* **1987**, *86*, 7230.
(10) Borisov, O. V.; Zhulina, E. B.; Birshtein, T. M. *J. Phys. II* **1994**, *4*, 913.
(11) Yamakov, V.; Milchev, A.; Borisov, O.; Dunweg, B. *J. Phys. Condens. Matter* **1999**, *11*, 9907.
(12) Hoeve, C. A. J. *J. Chem. Phys.* **1966**, *44*, 1505; *J. Polym. Sci.* **1970**, *C30*, 361.
(13) Hesselink, F. T. *J. Colloid. Interface Sci.* **1977**, *60*, 448.
(14) Van der Schee, H. A.; Lyklema, J. *J. Phys. Chem.* **1984**, *88*, 6661.
(15) Evers, O. A.; Fleer, G. J.; Scheutjens, J. M. H. M.; Lyklema, J. *J. Colloid. Interface Sci.* **1986**, *111*, 446.
(16) Blaakmeer, J.; Bohmer, M. R.; Cohen Stuart, M. A.; Fleer, G. J. *Macromolecules* **1990**, *23*, 2301.
(17) Bohmer, M. R.; Evers, O. A.; Scheutjens, J. M. H. M. *Macromolecules* **1990**, *23*, 2288.
(18) Varoqui, R.; Johner, A.; Elaissari, A. *J. Chem. Phys.* **1991**, *94*, 6873.
(19) Varoqui, R. *J. Phys. II*, **1993**, *3*, 1097.
(20) Borukhov, I.; Andelman, D.; Orland, H. *Europhys. Lett*, **1995**, *32*, 499.
(21) Chatellier, X.; Joanny, J.-F. *J. Phys. II* **1996**, *6*, 1669.
(22) Borukhov, I.; Andelman, D.; Orland, H. *Macromolecules* **1998**, *31*, 1665.
(23) Joanny, J.-F. *Eur. Phys. J. B* **1999**, *9*, 117.
(24) Netz, R. R.; Joanny, J.-F. *Macromolecules* **1999**, *32*, 9013.
(25) Solis, F. J.; de la Cruz, M. O. *J. Chem. Phys.* **1999**, *110*, 11517.
(26) Joanny, J.-F.; Castelnovo, M.; Netz, R. *J. Phys. Condens. Matter* **2000**, *12*, A1.
(27) Nguyen, T. T.; Grosberg, A. Yu.; Shklovskii, B. I. *Phys. Rev. Lett* **2000**, *85*, 1568; *J. Chem. Phys.* **2000**, *113*, 1110.
(28) Decher, G. *Science* **1997**, *277*, 1232.
(29) Hammond, P. T. *Curr. Opin. Colloid Interface Sci.* **1999**, *4*, 430.
(30) Rouzina, I.; Bloomfield, V. A. *J. Phys. Chem.* **1996**, *100*, 9977.
(31) Perel, V. I.; Shklovskii, B. I. *Physica A* **1999**, *274*, 446.
(32) Shklovskii, B. I. *Phys. Rev. Lett.* **1999**, *82*, 3268.
(33) Dobrynin, A. V.; Deshkovskii, A.; Rubinstein, M. *Phys. Rev. Lett.* **2000**, *84*, 3101.
(34) Lifson, S.; Katchalsky, A. *J. Polym. Sci* **1953**, *36*, 43.
(35) Alexandrowicz, Z.; Katchalsky, A. J. *Polym. Sci., Part A* **1963**, *1*, 3231.
(36) Alexander, S.; Chaikin, P. M.; Grant, P.; Morales, G. J.; Pincus, P.; Hone, D. *J. Chem. Phys.* **1984**, *80*, 5776.
(37) Hansen, J.-P. In *Observation, prediction and simulation of phase transitions in complex fluids*; Kluwert Academic Publishers: Dordrecht, The Netherlands, 1995.
(38) de Gennes, P.-G.; Pincus, P.; Brochard, F.; Velasco, R. M. *J. Phys. (Paris)* **1976**, *37*, 1461.
(39) de Gennes, P.-G. *Scaling Concepts in Polymer Physics*; Cornell University Press: Ithaca, NY, 1979.
(40) Dobrynin, A. V.; Colby, R. H.; Rubinstein, M. *Macromolecules* **1995**, *28*, 1859.
(41) The change in the free energy of the polyelectrolyte chain due to longitudinal fluctuations of the chain length δL may be obtained by expanding the elastic and electrostatic contributions to the free energy of the chain into Taylor series in the powers of $\delta L/L$.

$$\frac{\delta F(\delta L)}{kT} \approx \frac{\delta L^2}{a^2N} + \frac{l_B(fN)^2}{L^3}\delta L^2 \approx \frac{\delta L^2}{a^2N}$$

The estimate for the free energy variations due to displacement of the middle of a chain by the distance $R_\perp$ can be obtained by a similar procedure.

$$\frac{\delta F(R_\perp)}{kT} \approx \frac{R_\perp{}^2}{a^2N} + \frac{l_B(fN)^2}{L^3}R_\perp{}^2 \approx \frac{R_\perp{}^2}{a^2N}$$

The probability for quantity y to have a value in the interval from y to $y + dy$ is proportional to $\exp(-\delta F(y)/kT)$. This gives an estimate for the mean-square displacements in the longitudinal and transverse directions $\langle\delta L^2\rangle \approx \langle R_\perp{}^2\rangle \approx a^2N$.
(42) Safran, S. *Statistical Thermodynamics of Surface, Interfaces and Membranes*; Addison-Wesley: Reading, MA, 1994; p 187.
(43) Pincus, P. *Macromolecules* **1991**, *24*, 2912.
(44) A polyion interacting with its neutralizing backgroundis a standard approximation for a strongly correlated Wigner liquid. This result can be confirmed by resummation of the electrostatic attraction between polyions and the charged surface and by electrostatic repulsion from each other (see, for example: Bonsall, L.; Maradudin, A. A. *Phys. Rev. B* **1977**, *15*, 1959).
(45) Kaganer, V. M.; Mohwald, H.; Dutta, P. *Rev. Mod. Phys.* **1999**, *71*, 779.
(46) The loss of the entropic part of the free energy is on the order of kT up to logarithmic corrections. The logarithmic term is controlled by the bulk concentration of polyelectrolyte chains.
(47) Odijk, T. J. *Polym. Sci., Polym. Phys. Ed.* **1977**, *15*, 477.
(48) Skolnick, J.; Fixman, M. *Macromolecules* **1977**, *10*, 944.
(49) Khokhlov, A. R.; Khachaturian, K. A. *Polymer* **1982**, *23*, 1742.
(50) Li, H.; Witten, T. A. *Macromolecules* **1995**, *28*, 5921.
(51) Netz, R. R.; Orland, H. *Eur. Phys. J. B* **1999**, *8*, 81.
(52) Ha, B.-Y.; Thirumalai, D. *J. Chem. Phys.* **1999**, *110*, 7533.
(53) Tricot, M. *Macromolecules* **1984**, *17*, 1698.
(54) Reed, C. E.; Reed, W. F. *J. Chem. Phys.* **1991**, *94*, 8479.
(55) Forster, S.; Schmidt, M.; Antonietti, M. *J. Phys. Chem.* **1992**, *96*, 4008.
(56) Forster, S.; Schmidt, M. *Adv. Polym. Sci.* **1995**, *120*, 51.
(57) deNooy, A. E. J.; Besemer, A. C.; van Bekkum, H.; van Dijk, J.; Smit, J. A. M. *Macromolecules* **1996**, *29*, 6541.
(58) Nishida, K.; Urakawa, H.; Kaji, K.; Gabrys, B.;Higgins, J. S. *Polymer* **1997**, *38*, 6083.
(59) Tanahatoe, J. J. *J. Phys. Chem. B* **1997**, *101*, 10442.
(60) Beer, M.; Schmidt, M.; Muthukumar, M. *Macromolecules* **1997**, *30*, 8375.
(61) Barrat, J.-L.; Joanny, J.-F. *Europhys. Lett.* **1993**, *24*, 333.
(62) Bratko, D.; Dawson, K. A. *J. Chem. Phys.* **1993**, *99*, 5352.
(63) Ha, B.-Y.; Thirumalai, D. *Macromolecules* **1995**, *28*, 577.
(64) Seidel, C. *Ber. Bunsen-Ges. Phys. Chem.* **1996**, *100*, 757.
(65) Schafer, H.; Seidel, C. *Macromolecules* **1997**, *30*, 6658.
(66) Ullner, M.; Jonsson, B.; Peterson, C.; Sommelius, O.; Soderberg, B. *J. Chem. Phys.* **1997**, *107*, 1279.
(67) Micka, U.; Kremer, K. *Phys. Rev. E* **1996**, *54*, 2653.
(68) This definition of the adsorption/desorption transition corresponds to the ground-state dominance approximation. In this approximation, a polymer chain is considered to be adsorbed if there is a discrete level in the chain energetic spectrum well separated from its continuous spectrum. See for review: Grosberg, A. Yu.; Khokhlov, A. R. *Statistical Physics of Macromolecules*; AIP Press: Secaucus, NJ, 1994. See also refs 6, 7, 9, and 19.
(69) de Gennes, P.-G. *Adv. Colloid Interface Sci.* **1987**, *27*, 189.
(70) Durand, G.; Lafuma, F.; Audebert, R. *Prog. Colloid. Polym. Sci.* **1988**, *266*, 278.
(71) Froehling, P. E.; Bantjes, A. J. *Colloid Interface Sci.* **1977**, *62*, 35.

(72) Hendrickson, E. R.; Neuman, R. D. J. *Colloid Interface Sci.* **1986**, *110*, 243.
(73) Pelton, R. H. *J. Colloid Interface Sci.* **1986**, *111*, 475.
(74) Durand-Piana, G.; Lafuma, F.; Audebert, R. *J. Colloid Interface Sci.* **1987**, *119*, 474.
(75) Wang, T. K.; Audebert, R. *J. Colloid Interface Sci.* **1988**, *121*, 32.
(76) Davies, R. J.; Dix, L. R.; Toprakcioglu, C. *J. Colloid Interface Sci.* **1989**, *129*, 145.
(77) Shubin, V.; Linse, P. *J. Phys. Chem.* **1995**, *99*, 1285.
(78) Kawaguchi, M.; Kawaguchi, H.; Takahashi, A. *J. Colloid Interface Sci.* **1988**, *124*, 57.
(79) Bonekamp B. C. Ph.D. Thesis, Wageningen Agricultural University, The Netherlands 1984.
(80) Marra, J.; van der Schee, H. A.; Fleer, G. J.; Lyklema, J. In *Adsorption in Solutions*; Ottiwel, R., Rochester, C. H., Smith, A. L., Eds.; Acad. Press: San Diego, CA, 1983; p. 245.
(81) Dobrynin, A. V.; Rubinstein, M.; Obukhov, S. P. *Macromolecules* **1996**, *29*, 2974.
(82) Dobrynin, A. V.; Rubinstein, M. *Macromolecules* **1999**, *32*, 915.
(83) Castelnovo, M.; Sens, P.; Joanny, J.-F *Eur. Phys. J. E* **2000**, *1*, 115.
(84) Balazs, A. C.; Singh, C.; Zhulina, E.; Pickett, G.; Chern, S. S.; Lyatskaya, Y. *Prog. Surf. Sci.* **1997**, *55*, 181.
(85) Solis, F. J.; Olvera de la Cruz, M. *Macromolecules* **1998**, *31*, 5502.
(86) Micka, U.; Holm, C.; Kremer, K. *Langmuir* **1999**, *15*, 4033.
(87) Lyulin, A. V.; Dunweg, B.; Borisov, O. V.; Darinskii, A. A. *Macromolecules* **1999**, *32*, 3264.
(88) Chodanowski, P.; Stoll, S. *J. Chem. Phys.* **1999**, *111*, 6069.
(89) Micka, U.; Kremer, K. *Europhys. Lett* **2000**, *49*, 189.

MA0013713